Density functional study of beryllium clusters, with gradient correction

LETTER TO THE EDITOR

Density functional study of beryllium clusters, with gradient correction

Jinlan Wang[1,2]**, Guanghou Wang**[1] **and Jijun Zhao**[3]

[1] National Laboratory of Solid State Microstructures and Department of Physics,
Nanjing University, Nanjing 210093, People's Republic of China
[2] Department of Physics, Guangxi University, Nanning 530004, People's Republic of China
[3] Department of Physics and Astronomy, University of North Carolina at Chapel Hill,
Chapel Hill, NC 27599-3255, USA

E-mail: ghwang@nju.edu.cn (Guanghou Wang) and zhaoj@physics.unc.edu (Jijun Zhao)

Abstract
By using density functional theory with Becke–Lee–Yang–Parr (BLYP)
gradient correction, we have studied the structural and electronic properties
of beryllium clusters up to 21 atoms. The theoretical calculations successfully
reproduce the experimental bond length and vibrational frequency of the Be_2
dimer and the overestimation of the binding energy is significantly reduced
compared to that in previous theoretical work. The Be_n clusters with $n =
4, 10, 17$ show particularly high stability, consistently with the electron shell
model. The size evolution of the electronic properties from van der Waals to
covalent and bulk metallic behaviour in Be clusters is discussed.

In recent years, metal clusters have been intensively studied both theoretically and exp-
erimentally [1–4]. It is of fundamental interest to illustrate the evolution from molecular
states to bulk metallic character in metal microclusters as the size increases. It is well known
that very small divalent metal clusters are van der Waals-like; in these clusters the atoms have
s^2 closed-shell atomic configurations like helium and are weakly bound. On the other hand,
the bulk solids of these elements are metallic because of the overlap between s and p bands.
Therefore, probing the transition from van der Waals to metallic bonding in divalent metal
clusters is an interesting topic in cluster physics [5–19].

Although there are several theoretical works on beryllium clusters [5–11], experiments
have been limited to the Be_2 dimer [22]. Among those studies, the accurate quantum chemistry
calculations are usually limited to small cluster size, i.e., $n \leqslant 8$ [5, 9–11]. The structures
of larger beryllium clusters have been determined by Car–Parrinello simulation based on
the plane-wave pseudopotential technique with the local density approximation (LDA) [7].
However, a comparative study on the divalent metal dimers using different density functional
approximations has shown that the gradient correction is significant as regards determining the

ground-state properties of such finite systems [8]. For instance, LDA calculation has predicted the atomization energy of Be_2 as 0.60 eV. After a Becke-type gradient correction was included, it was reduced to 0.39 eV, which is closer to the experimental value of 0.11 eV. Since the LDA used in most previous works might overestimate the cohesion of small van der Waals-like Be_n clusters, a comprehensive DFT study including proper gradient correction is essential to investigate the size evolution towards bulk metallic behaviour of beryllium clusters.

In the past decade, simulated annealing (SA) based on density functional calculation has become a well-established technique for determining the ground-state structures of atomic clusters. However, the presence of numerous isomers in configuration space leads to a rather high computational cost for the clusters with $n > 10$. As an alternative, using a first-principles many-body potential fitted for Be clusters [6], we generate a number of isomers from a genetic algorithm (GA) simulation [20, 21]. Further DFT optimizations are applied to these empirical isomers to determine the lowest-energy structures. The essential idea of the current scheme is that of dividing the phase space into a number of regions, each of which can be represented by these local isomers from empirical GA simulations. Although the energies and structural parameters of these isomers may not be described very accurately by the empirical potential, these minima might provide a reasonable sampling of the DFT phase space. Finally, the global minimum configuration at DFT level can be obtained with considerably less computational cost.

In this work, density functional self-consistent-field (SCF) electronic structure calculations are performed by using the DMol package [24]. The density functional is treated with Becke's [25] gradient-corrected exchange potential and the Lee–Yang–Parr gradient-corrected correlation potential (BLYP) [26]. Geometry optimizations are performed by the Broyden–Fletcher–Goldfarb–Shanno (BFGS) algorithm with a convergence criterion of 10^{-3} au for the gradient and displacement, and 10^{-5} au for the total energy and electronic density.

The geometrical structures of the ground state and some metastable isomers of small beryllium clusters ($n = 3$–10) are shown in figure 1. For the Be_2 dimer, our BLYP calculation predicts the bond length $r = 2.47$ Å, binding energy $E_b = 0.23$ eV and vibrational frequency $\omega = 314$ cm^{-1}, which compare well with experimental data ($r_e = 2.47$ Å, $E_{be} = 0.11$ eV, $\omega_e = 276$ cm^{-1}) [22, 27]. In particular, the overestimation of the atomization energy by the
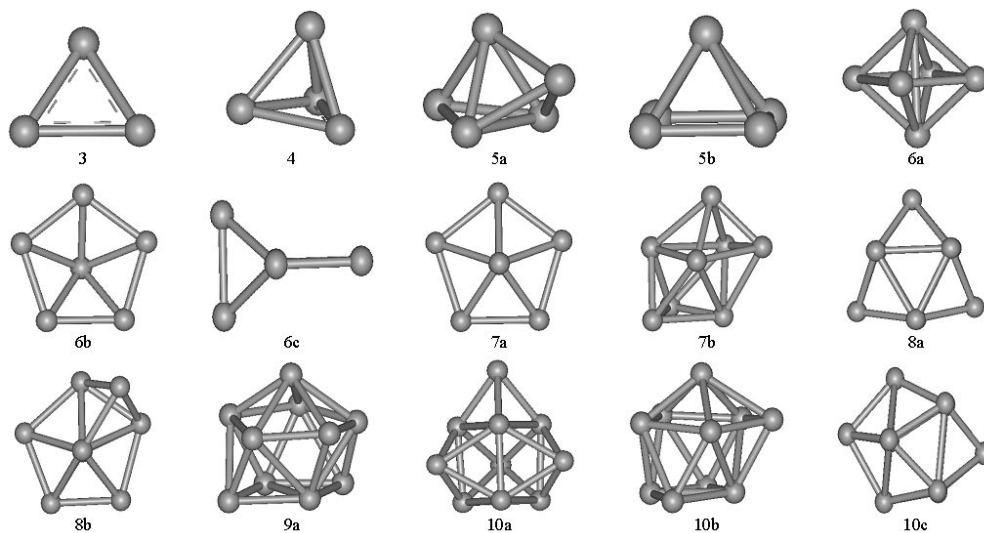

Figure 1. Lowest-energy and metastable structures for Be_n ($n = 3$–10) clusters.

LDA is considerably reduced [8]. Since the present BLYP scheme has described the Be_2 dimer satisfactorily, one may expect it to provide accurate predictions for the larger beryllium clusters. The structures and binding energies of small clusters ($n = 2$–8) in our calculations are compared with previous theoretical results in table 1. The present binding energies are very similar to B3LYP/6-311G(3df) results, while LDA methods overestimate the cohesion significantly.

Table 1. Binding energies per atom E_b (eV) and bond lengths (Å) (in brackets) for small Be_n clusters with $n = 2$–8. The bond lengths for the clusters with $n = 7, 8$ are given as averages of nearest-neighbour distances. (a) to (d) label previous *ab initio* calculations. (a): B3LYP/6-311G(3df) [13]; (b): LSDA [12]; (c): LSDA with a GTO(9s, 3p) basis set [5]; (d): MP4/6-311G* for energies of $n = 3$–5 clusters, MP4/6-311G* for the energy of the $n = 6$ cluster, MP2/6-311G* for bond lengths of $n = 3$–5 clusters, MP4/6-311G* for the bond length of the $n = 6$ cluster [9].

n	Symmetry	This work	(a)	(b)	(c)	(d)
2	$D_{\infty h}$	0.11(2.47)	0.10(2.48)	0.18(2.57)	0.18(2.57)	
3	D_{3h}	0.48(2.18)	0.47(2.16)	0.57(2.23)	0.53(2.29)	0.31(2.24)
4	T_d	1.03(2.05)	1.06(2.03)	1.18(2.08)	1.09(2.14)	0.90(2.09)
5	D_{3h}	1.14(2.01, 2.08)	1.16(1.98, 2.04)	1.26(2.07, 2.06)	1.22(2.06, 2.13)	1.06
6	C_{2v}	1.13(1.88, 2.05)	1.19(2.12)	1.21(2.09)	1.59	0.99
7	D_{5h}	1.26(2.12)	1.33(2.01)			
8	D_{3d}	1.42(2.12)	1.43(2.05)			

For the Be_3 trimer, the lowest-energy structure is obtained as an equilateral triangle structure with bond lengths of 2.18 Å. The bond length of Be_3 is considerably shorter than that of the Be_2 dimer and there is a substantial increase in binding energy from Be_2 to Be_3. The increase of cohesion between Be atoms continues up to $n = 4$–6. In the case of Be_4, a tetrahedron with bond lengths of 2.05 Å is obtained while the planar rhombus is not even a stable isomer upon relaxation. The lowest-energy structure found for Be_5 is a trigonal bipyramid (5a) with a 2.01 Å short bond and a 2.08 Å long bond, which has lower energy ($\Delta E = 0.67$ eV) than a square pyramid (5b). For Be_6, the most favourable structure is an octahedron (6a) with average bond lengths of 2.02 Å (6a), which is about 0.39 eV lower in energy than the pentagon (6b) and 0.44 eV lower in energy than the 'Y-type' structure (6c). The present results for Be_6 are consistent with LSD studies [10] but different from B3LYP/6-311G results, in which the lowest-energy structure is predicted as a distorted C_{2v} structure [11].

However, the trend of bond-length decrease with cluster size does not continue to Be_7. The bond lengths increased to 2.12 Å for the seven-atom beryllium cluster. For Be_7, the pentagonal bipyramid (7a) is more stable than a capped octahedron structure (7b) by $\Delta E = 0.24$ eV; this result was also obtained by other theoretical calculations [9, 11]. For the clusters with $n \geqslant 7$, the average bond lengths are very close to the nearest-neighbour distance in bulk metallic beryllium. These findings may imply that the bonding in these Be_n clusters is no longer van der Waals-like. Kawai and Weare have also predicted the sp hybridization to converge to the bulk behaviour by $n = 6$ [7]. The distorted bicapped octahedron structure (8a) is more stable than a capped pentagonal bipyramid (8b) for Be_8. The most favourable geometry for Be_9 is a tricapped trigonal prism (9a) with C_{3v} symmetry. For Be_{10}, the tetracapped trigonal prism (10a) is the most stable structure while the bicapped square antiprism (10b) and tricapped pentagon (10c) are local minima with $\Delta E = 0.15$ eV and 0.22 eV, respectively.

The more compact configurations are found for the beryllium clusters with $n = 11$–21 as shown in figure 2. These structures are quite different from noble-gas clusters. For Be_{11} and Be_{12}, the lowest-energy structures can be taken as a cage-like distorted icosahedron structure with a missing apex atom and an icosahedral cage, respectively. In fact, the structures of Be_n
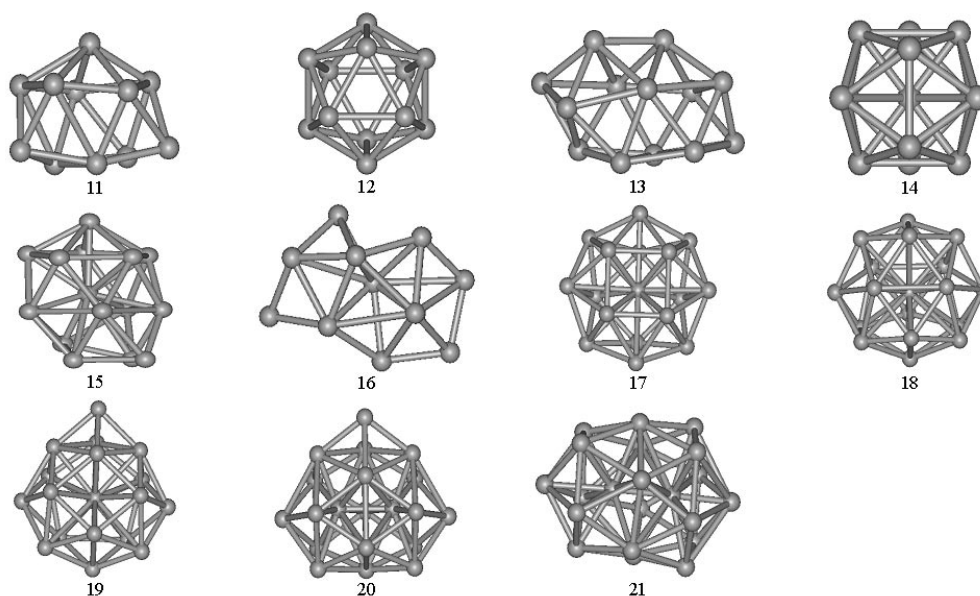
Figure 2. Lowest-energy and metastable structures for Be_n ($n = 11$–21) clusters.

clusters with $n = 7$–12 are quite similar to silicon or germanium semiconductor clusters. Such similarity might imply some covalency of the bonding character in these clusters. The most stable structure found for Be_{13} is neither an icosahedron nor a face-centred cube structure but a prolate cage including several interpenetrating pentagonal bipyramids. This structure is different from those of noble-gas and semiconductor clusters, which might suggest the onset of metal bonding in the clusters. For Be_{14}, an additional atom capping a distorted icosahedron yields the lowest-energy structure. Each of Be_{15} and Be_{16} can also be understood as a severely distorted icosahedron plus two or three capping atoms. However, the icosahedral growth pattern does not continue for the Be_n clusters with $n = 17$–19. In particular, the Be_{19} cluster is not found as a double icosahedron. The most stable structures for Be_{17-19} are ellipsoids comprised of tetrahedral, pentagonal and hexagonal structures each with a central atom. These results also indicate that the bonding in these Be clusters is different from van der Waals or covalent. The icosahedral packing appears again in Be_{20} and Be_{21}, which grows on the basis of a double icosahedron with one or two capping atoms.

The binding energy per atom E_b of Be_n clusters as a function of cluster size n is plotted in figure 3(a). Two sections of rapid increase in binding energy are found in the ranges $n = 2$–4 and 6–10. The first rapid increase of binding energy for the clusters with $n = 2$–4 corresponds to the significant decrease of the average bond length. The second increase may be related to the appearance of more highly coordinated structures. For $n \geqslant 10$, the binding energies per atom increase smoothly. Our present results on the size dependence of the cluster binding energy agree well with previous theoretical calculations [7].

On the basis of the above results, we can discuss the size evolution behaviour for beryllium clusters from molecular states to covalent and bulk metallic states. In small beryllium clusters, the 2s valence electrons are dominant in determining the cluster properties. Since the electronic configuration of the beryllium atom ($2s^2$) is similar to that of helium, it is natural that small Be_n clusters with $n = 2$–6 exhibit certain noble-gas-like behaviours. As the cluster size increases, the hybridization between the 2s states and unoccupied 2p states leads to some covalency of
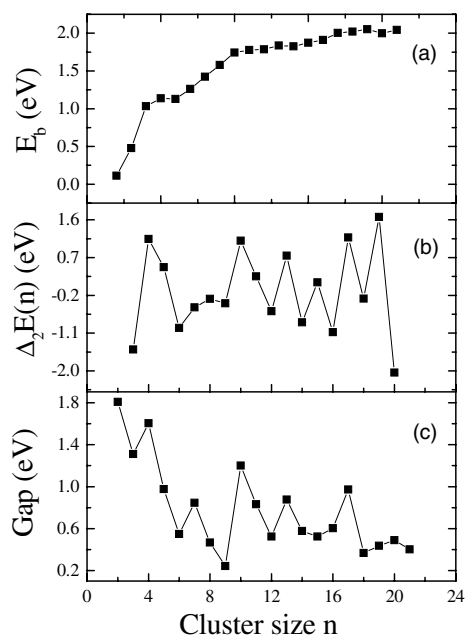
Figure 3. (a) Binding energy per atom (E_b/n) versus cluster size for Be_n; (b) second difference of cluster energies $\Delta_2 E(n) = E(n-1) + E(n+1) - 2E(n)$ as a function of cluster size n for $n = 2$–21; (c) HOMO–LUMO (see the text) gap (eV) versus cluster size for Be_n.

the bonding in the clusters with $n = 7$–12. The further development of orbital hybridization may cause the overlap of s and p states and metallic cohesion. Our present calculations suggest that the transition from covalent bonding to metallic bonding occurs around $n = 13$.

In figure 3(b), we present the second difference of cluster total energies defined by $\Delta_2 E(n) = E(n+1) + E(n-1) - 2E(n)$ (where $E(n)$ is the total energy of the Be_n cluster). It is well known that $\Delta_2 E(n)$ is a sensitive quantity that reflects the stability of clusters. As shown in figure 3(b), particularly high peaks for $\Delta_2 E(n)$ are found at $n = 4, 10, 13, 15, 17, 19$, indicating that the clusters with these values of n are more stable than their neighbouring clusters. The present results agree well with previous LDA simulation results (maxima at $n = 4, 10, 17$) [7]. The particularly high stability of Be_4, Be_{10}, Be_{17} can be understood in view of the magic numbers of total valence electrons of 8, 20, 34 predicted by the electronic shell model [1,2]. On the other hand, the magic numbers at $n = 13, 19$ may be due to the atomic structure effect. For example, the prolate cage with interpenetrating pentagonal bipyramids for Be_{13} may enhance the stability of the ground-state structure.

In figure 3(c), we present the energy gap between the highest occupied molecular orbital (HOMO) and lowest occupied molecular orbital (LUMO) for Be_n clusters. A large (small) HOMO–LUMO gap generally corresponds to a closed-shell (open-shell) electronic configuration. In figure 3(c), the HOMO–LUMO gap is particularly large for Be_2, Be_4, Be_{10} and Be_{17} (1.81 eV, 1.61 eV, 1.2 eV and 0.97 eV, respectively), indicating that these clusters have closed-shell electronic configurations with enhanced stability. These large HOMO–LUMO gaps can be associated with the magic numbers of total valence electrons of 8, 20, 34 predicted by the electronic shell model [1,2]. The observation of electron shells in Be_n clusters indicates that a Be_n cluster containing more than a few atoms may already demonstrate some metallic-like features that are similar to those shown by the alkali metal clusters.

In summary, the geometrical and electronic properties of beryllium clusters have been studied by using a BLYP density functional calculation. The relative stability, binding energies, HOMO–LUMO gaps and densities of states demonstrate high stability at the sizes $n = 4$, 10, 17 with closed electronic shells. Nonmetal-to-metal transitions in the Be clusters are obtained. In small beryllium clusters, the closed-shell configurations lead to certain noble-gas-like behaviours for the sizes $n = 2$–6. As the cluster size increases, the hybridization of atomic orbitals leads to the transition from van der Waals to covalent bonding at about the size $n = 7$ and to metallic bonding at around $n \geqslant 13$.

References

 [1] Moskovits M 1991 *Annu. Rev. Phys. Chem.* **42** 465
 [2] de Heer W A 1993 *Rev. Mod. Phys.* **65** 611
 [3] Haberland H (ed) 1995 *Clusters of Atoms and Molecules I* (Berlin: Springer)
 [4] Kresin V V and Knight W D 1998 *Z. Phys. Chem.* **203** 57
 [5] Khanna S N, Reuse F and Buttet J 1988 *Phys. Rev. Lett.* **61** 535
 [6] Barojas E B and Khanna S N 1988 *Phys. Rev. Lett.* **61** 1477
 [7] Kawai R and Weare J H 1990 *Phys. Rev. Lett.* **65** 80
 [8] Ortiz G and Ballone P 1991 *Z. Phys.* D **19** 169
 [9] Sudhakar P V and Lammertsma K 1993 *J. Chem. Phys.* **99** 7929
[10] Kolchin A M and Hall R W 2000 *J. Chem. Phys.* **113** 4083
[11] Beyer M K *et al* 2000 *Chem. Phys.* **262** 15
[12] Rademann K 1991 *Z. Phys.* D **19** 161
     Kaiser B and Rademann K 1992 *Phys. Rev. Lett.* **69** 3204
[13] Ruppel M and Rademann K 1992 *Chem. Phys. Lett.* **197** 280
     Rademann K, Ruppel M and Kaiser B 1992 *Ber. Bunsenges. Phys. Chem.* **96** 1204
     Rademann K 1993 *J. Non-Cryst. Solids* **156–158** 794
[14] Pastor G M, Stampfli P and Bennemann K H 1988 *Europhys. Lett.* **7** 419
     Pastor G M, Stampfli P and Bennemann K H 1989 *Z. Phys.* D **12** 365
[15] Kumar V and Car R 1991 *Phys. Rev.* B **44** 8243
[16] Gong X G, Zheng Q Q and He Y Z 1993 *Phys. Lett.* A **181** 459
[17] Zhao J, Chen X and Wang G 1994 *Europhys. Lett.* **28** 311
[18] Boutou V, Dorget M A L, Allouche A R, Bordas C and Chevaleyre J 1997 *Z. Phys.* D **40** 448
[19] Flad H J, Schautz F, Wang Y, Dolg M and Savin A 1999 *Eur. Phys. J.* D **6** 243
[20] Deaven D M and Ho K M 1995 *Phys. Rev. Lett.* **75** 288
     Deaven D M, Tit N, Morris J R and Ho K M 1996 *Chem. Phys. Lett.* **256** 195
[21] Luo Y H, Zhao J J, Qiu S T and Wang G H 1999 *Phys. Rev.* B **59** 14 903
     Wang B L, Yin S Y, Wang G H, Buldum A and Zhao J J 2001 *Phys. Rev. Lett.* **86** 2046
[22] Huber K P and Herzberg G 1979 *Constants of Diatomic Molecules (Molecular Spectra and Molecular Structure vol 4)* (Princeton, NJ: Van Nostrand)
[23] Perdew J P and Wang Y 1992 *Phys. Rev.* B **45** 13 244
[24] DMOL is a density functional theory (DFT) package, based on the atomic basis, distributed by MSI;
     Delley B 1990 *J. Chem. Phys.* **92** 508
[25] Becke A D 1988 *Phys. Rev.* A **38** 3098
[26] Lee C, Yang W and Parr R G 1988 *Phys. Rev.* B **37** 785
[27] Bondybey V E 1984 *Chem. Phys. Lett.* **109** 436